Applied Energy 334 (2023) 120651

Contents lists available at ScienceDirect

Applied Energy

journal homepage: www.elsevier.com/locate/apenergy

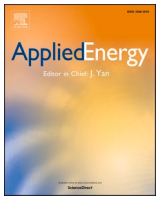

Performance evaluation of modified compound organic Rankine-vapour compression cycle with two cooling levels, heating, and power generation

Ali Khalid Shaker Al-Sayyab [a,b], Adrián Mota-Babiloni [a,*], Joaquín Navarro-Esbrí [a]

[a] ISTENER Research Group, Department of Mechanical Engineering and Construction, Universitat Jaume I, Av. de Vicent Sos Baynat s/n, 12071 Castelló de la Plana, Spain
[b] Basra Engineering Technical College (BETC), Southern Technical University, Basra, Iraq

HIGHLIGHTS

- The novel ORC-VCE combination has an average 18% COP increase.
- The proposed R1234ze(E) system can increase power generation by 58% more than a conventional ORC.
- The system has a wide operation range of ground source temperatures with higher thermal efficiency.
- Additional heat exchangers increase energy efficiency and waste heat valorisation potential.

GRAPHICAL ABSTRACT

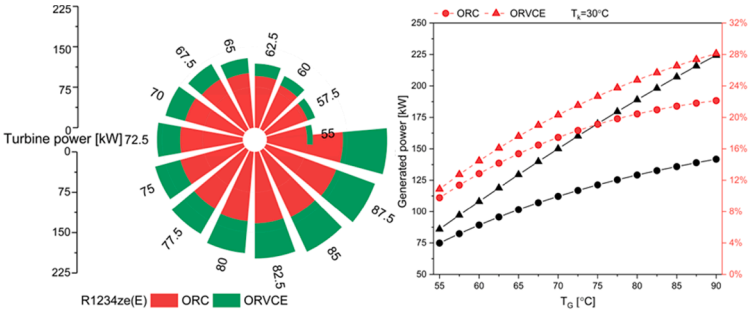

a) b)

ARTICLE INFO

Keywords:
Ground source
Heat recovery
organic Rankine cycle (ORC)
Ejector
Vapour compression system
low global warming potential (GWP)

ABSTRACT

This work analyses a novel combined organic Rankine-compound ejector vapour compression cycle for power, cooling and heating production using a low-grade ground heat source as the primary heat source. Ultra-low global warming potential working fluids (R1234ze(E), R1243zf, and R1234yf) and parameters quantifying energy and exergy efficiency are considered. The system can be adapted to three operating modes, depending on the ground source temperature, ranging from 55 to 90 °C: power-cooling, power-heat pump heating, and power-ground source heating. The results indicate that this system notably increases the overall performance of all investigated refrigerants. Compared to conventional organic Rankine and vapour compression cycles (ORC and VCC), the R1234ze(E) power-cooling mode shows the highest coefficient of performance (COP) increase, 18 %. Besides, including a recapture heat exchanger for condenser waste heat recovery can increase power generation by 58 %. At ground source temperatures up to 65 °C, power generation and thermal efficiency increased in the power-heating mode due to the absence of the compressor power consumption. The exergy efficiency follows the ground source temperatures for all modes. In power-ground source heating mode, the exergy efficiency notably increased due to the absence of the heat pump exergy destruction.

* Corresponding author.
E-mail addresses: ali.alsayyab@stu.edu.iq (A.K.S. Al-Sayyab), mota@uji.es (A. Mota-Babiloni), navarroj@uji.es (J. Navarro-Esbrí).

https://doi.org/10.1016/j.apenergy.2023.120651
Received 14 July 2022; Received in revised form 2 January 2023; Accepted 5 January 2023
Available online 23 January 2023

Nomenclature

$\dot{E}x$	Exergy rate (kJ s^{-1})
h	Specific enthalpy (kJ kg^{-1})
$\dot{m}$	Refrigerant mass flow rate (kg s^{-1})
P	Pressure (bar)
$\dot{Q}$	Heat transfer rate (kW)
s	Specific entropy (kJ kg^{-1} K^{-1})
SI	Sustainability index (-)
T	Temperature (°C)
UA	Overall heat transfer coefficient (kW K^{-1})
$\dot{W}$	Power consumption or generation (kW)

Greek symbols

η	Efficiency (-)
ε	Effectiveness (-)
μ	Entrainment ratio (-)
ρ	Density (kg m^{-3})

Subscripts

b	Bulk
C	Compressor, cooling mode
cri	Critical condition
D	Diffuser, Discharge
des	Destruction
e	Evaporator
EC	Economic
ej	Ejector
ek	Evaporative-condenser
em	Electromechanical
exp	Expansion valve
FT	Flash tank
0	Dead state conditions
G	Ground source
h	Hot stream, heating mode
HT	High temperature
HX	Heat exchanger
HP	Heat pump
in	Inlet
is	Isentropic
II	Second law of Thermodynamics
K	Condenser
L	Cold stream
LT	Low temperature
M	Mixing
out	Outlet
P	Pump
pn	Primary nozzle
r	Refrigerant, ratio
R	Recapture
sn	Suction nozzle
T	Turbine
th	Thermal
v	Volumetric

Abbreviatures

COP	Coefficient of Performance (-)
CO_2-eq	Equivalent carbon dioxide emissions
ASHRAE	The American Society of Heating, Refrigerating and Air-Conditioning Engineers
EES	Engineering Equation Solver
GWP	Global Warming Potential (100 years time horizon)
GHG	Greenhouse gas
HFC	Hydrofluorocarbon
ODP	Ozone Depletion Potential
ORC	Organic Rankine cycle
ORC-VCC	Organic Rankine cycle - vapour compression cycle
ORVCE	Organic Rankine cycle - vapour compression ejector cycle
MORVC	Modified organic Rankine cycle - vapour compression cycle
NBP	Normal Boiling Point (°C)
RORC	Regenerative organic Rankine cycle

1. Introduction

Approximately half of the net electricity generated in the European Union (EU) comes from fossil fuels (natural gas, coal, and oil) [1]. In November 2018, the European Commission (EC) released decarbonising strategies to achieve "carbon neutrality" by 2050 [2]. In September 2021, the EC increased restrictions on the EU's 2030 greenhouse gas (GHG) emission target from 40 % to 50 % (below 1990 levels), with 32.5 % energy efficiency improvement and 32 % renewable energy share.

Electricity and heating processes represent the primary source of global emissions (25 % of 2010 global GHG emissions) [3]. As a result of the global mean surface temperature increase due to GHG emission, according to a European Commission report, by 2030, heating and cooling electricity demand will increase by 35 % compared to 2012 [4]. Electricity generation should reach net-zero emissions globally in 2040 and provide almost half of total energy consumption [5]. Therefore, green electricity generation and highly efficient heating and cooling systems represent future challenges.

This requires electricity based on solar, hydropower, wind, and ground sources. Ground source energy is a reliable, sustainable, cost-effective (lowest cost per kWh among all renewable energy sources), and environmentally friendly energy source. It is a constant energy source, contrary to wind and solar, with a capacity factor (ratio of actual power production to production potential) of up to 96 % [6]. Moreover, ground-source power plants have an average emission of 122 kg CO_2-eq per MWh [7].

Organic Rankine Cycles (ORC) have evolved until being considered promising technologies in recovering low-grade thermal energy. Their working fluids can operate at moderate pressure and with low-cost materials. Moreover, ORC can be constructed even for small-scale applications [8,9]. Attending to the Carnot efficiency, only 10 % to 20 % of the input heat was utilised by ORC [10]. This causes extremely low electric efficiency and limits large-scale deployment [11]. In recent years, the ORC energy performance has been evaluated with different low global warming potential (GWP) refrigerants. Yang et al. [12] compared R1224yd(Z), R1233zd(E), R1234ze(Z), R245fa, and R1336mzz(Z). R1224yd(Z) thermal efficiency was 11.2 % higher than R245fa. Javanshir et al. [13] simulated a regenerative ORC (RORC) with 14 dry refrigerants. The regenerator increased thermal efficiency while not affecting net power generation. The highest specific work was obtained with butane (R600), R600a (isobutane), and R113. Liu et al. [14] evaluated energy and exergy ORC performance using twelve refrigerants R1225ye(Z), R1234yf, R1234ze(E), R1234ze(Z), R1243zf, R1225ye(E), R1225zc, R1234ye(E) with a ground source heat source. R1234yf fits with low ground source temperatures (around 120 °C), while R1234ze (Z) presents the highest system efficiency (8.9 %) at high supply temperatures. Molés et al. [15] theoretically evaluated the ORC performance using low GWP refrigerants R1234yf and R1234ze(E) as alternatives for R134a. R1234ze(E) presents a 13.9 % net efficiency increase compared to R134a, while R1234yf results in the lowest values. Li et al. [16] compared R1234ze(E) and R600a as R134a alternatives for

subcritical and transcritical ORC conditions and using hot water as a heat source. The temperature range of 100 to 160 °C is suitable for subcritical operation, whereas 160 to 200 °C for transcritical conditions. R1234ze(E) shows the highest net power generation. Zhi et al. [17] optimised energy and exergy performance for R1234ze(E) transcritical ORC. Turbine and pump efficiency and the inclusion of a regenerator remarkably impact system performance. Zhang et al. [18] numerically evaluated ORC performance (net power generation, thermal efficiency, and condenser load) using R1234yf, R1234ze(E) and R1336mzz(Z). R1234ze(E) resulted in the highest performance for transcritical cycles.

A few experimental studies evaluated the ORC performance with different waste heat sources. Navarro-Esbrí et al. [19] proved that an R1224yd(Z) drop-in replacement increases net efficiency by 7.7 % over R245fa small-scale ORC. Haghparast et al. [20] predicted that ejectors in R245fa ORCs increase power generation. Furthermore, a 6 % higher ejector normal shock section diameter increased power generation by 13 %. Rijpkema et al. [21] evaluated an R1233zd(E) ORC with waste heat recovery from diesel engine cooling. At 8 bar and 92 ℃, the thermodynamic efficiency is between 1.1 % and 1.8 %, with a maximum expander power generation of 0.7 % relative to the engine power consumption. Li et al. [8] proved in a 3 kW R245fa ORC that a higher waste heat mass flow rate decreases heat recovery effectiveness.

ORC combined with vapour compression cycles (ORC-VCC) to cool and generate electricity or heat and electricity has been proposed. Molés et al. [22] showed that the R1234ze(E) presents a slightly higher energy performance than R1336mzz(Z). In contrast, if the latter is used as the ORC working fluid, it results in modestly higher thermal and significantly higher electrical efficiency. Yu et al. [23] concluded that ORC-VCC does not always increase system energy performance. Javanshir et al. [24] considered ground source water a low-temperature heat source. Both turbine and boiler represent the highest exergy destruction source, whereas R22 and R143a present the highest energy and exergy efficiency.

A few studies have investigated the ORC-VCC system efficiency by connecting various waste heat recovery sources. Liu et al. [25] theoretically evaluated a built-in evaporator, which increased thermal efficiency and waste heat recovery by 6.4 % and 1.2 % compared to a traditional system. R1233zd(E) showed the highest thermal and exergy efficiency, 32.2 % and 38.9 % (other refrigerants considered were R601, R365mfc, R245ca, R1233zd(E), R1224yd(Z), R600, R600a, R290, and R114). Ashwni et al. [26] simulated an ORC-VCC with a flash tank, waste heat from solar collectors, and a biomass burner operating with different refrigerants (hexane, heptane, octane, nonane, and decane).

Similarly, only a few works have studied the increase of the ORC-VCC performance by employing additional cycle components. Yang et al. [27] showed that if an ejector is added to the VCC, an exergy and thermal efficiency increase of 10.3 % and 10.8 % is achieved with an R600a/R601 mixture (40 %/60 %). Pektezel et al. [28] connected the ORC to two VCC (single and dual evaporators) using R134a, R1234ze(E), R227ea, and R600a. The boiler and compressor represent the highest exergy destruction source. The evaporator and boiler temperature increase and condenser temperature decrease results in a higher system COP.

Studies have suggested that ORC-VCC efficiency can be enhanced by using various waste heat recovery sources. Liao et al. [29] theoretically evaluated the energy-exergy performance of trigeneration ORC-VCC actuated by coal-fired plant bottom slag waste heat, using (R227ea, R1234ze(E), R600, R245fa, R123, R601a, Hexane, Cyclohexane, Heptane) as working refrigerants. The study observed that the chilled water mass flow rate has a positive influence on the system COP and refrigeration capacity while having a reduction influence on the total exergy production rate. The heptane-R601a pair shows the highest energy and exergy performance. Nasir et al. [30] performed an energy and exergy evaluation of the combined ORC-VCC for Simultaneous heating, cooling and power generation using Biomass waste heat as an ORC heat source. The study indicated that the heat capacity rate and system exergy destruction are directly proportional to boiler saturation temperature. The system can provide 30 kW of cooling and 528 kW of heating. Zhar et al. [31] carried out an energy-exergy analysis for combined ORC-VCC for cooling, and power generation purposes with exhaust gases waste heat utilisation as an ORC heat source. With R123, R11 and R113 as the working fluid. The system with R123 shows the highest energy and exergy efficiency, 10 and 53 %, respectively. Eisavi et al. [32] presented a compound ORC-VCC and PV/T system for power and water distillation actuated by the geothermal and PV/T waste heat with R245fa. The system can produce 141 $m^3.d^{-1}$ distilled water by consuming 38.7 kW.

Another way of increasing ORC efficiency is by combining subsystems like heat pumps, absorption chillers, and solar collectors. Sun et al. [33] simulated an ORC combined with an absorption cycle and R113 ejector refrigeration cycle to recover waste heat from low-temperature flue gas. The ORC evaporation temperature decreases exergy efficiency. The combined system performs better until an evaporating temperature of 153 ℃. Wang et al. [34] performed an energy exergy performance analysis for solar actuated combined ORC-absorption system for power and cooling. The system produces 6.4 kW refrigeration capacity and 1 kW electricity with an ARC COP of 0.8, while overall exergy efficiency ranges from 56 % to 74 %. Roumpedakis et al. [35] did an energy-exergy evaluation for flue gas waste heat actuated combined ORC-ARC for power and cooling purpose. The study concludes that ORC-ARC has less exergy destruction and performs better than the combined ORC-VCC systems. Lu et al. [36] evaluated the energy-exergy performance of combined ORC-ARC using boiler flue gas waste heat. The results proved that the waste heat recovery heat exchanger increases energy and exergy efficiency by 37.7 % and 35.6 %, respectively. Zheng et al. [37] theoretically investigated a solar-powered ORC-VCC using five zeotropic mixtures and eight pure refrigerants. Dry fluids show more advantages than wet because of a higher specific heat value, being R600a the most promising pure refrigerant. Saini et al. [38] proposed a trigeneration system (power, cooling, and heating) consisting of evacuated tube collectors coupled with thermal energy storage, ORC, ejector refrigeration cycle, and water heater.

A few studies experimentally evaluated the potential of combined ORC-VCC. Demierre et al. [39] used R134a in a 20 kW prototype in which the compressor-turbine unit represents the most critical component. Liang et al. [40] used R245fa and R134a for a lab-scale ORC-VCC. At a 95 ℃ heat source temperature, the system produces 1.8 kW cooling power at (− 4 ℃), with 18 % overall heating-to-cooling efficiency. Grauberger et al. [41] combined an R1234ze(E) ORC and a 264 kW chiller. The condenser glycol outlet temperature had the most significant impact on the overall performance. They measured an overall COP, ORC thermal efficiency, and VCC COP of 0.56, 7.7 %, and 5.25, respectively.

To improve the thermo-economic performance of combined ORC-VCC systems, many studies focused on single and multi-objective optimisation by employing the most powerful technique genetic method. Akbari Kordlar et al. [42] carried out an exergeoconomic analysis and optimisation for combined ORC-ARC for power and cooling purpose. The optimisation result indicated that the optimum energy and exergy performance increased total cost by around 20.4 % and 24.32 %. Modifications should be prioritised for the turbine, condenser, and absorber. Xia et al. [43] performed a multi-objective optimisation for a low-grade heat source ejector-driven transcritical CO_2 Rankine cycle. The optimisation result indicated that the system costs and benefits go hand in hand. Salim et al. [44] presented a multi-objective optimisation of a combined ORC-VCC using R245ca and R236ea as working fluid. According to the optimisation results, the R245ca shows the highest performance associated with a high cost, whereas R236ea shows the lowest. Cao et al. [45] used a genetic algorithm to optimise the performance of a flue gas waste heat-actuated combined ORC-ejector refrigeration system. The optimisation results improve the system's thermal and exergetic efficiencies by 28 % and up to 10 %, respectively. Santiago et al. [46] did an energy-exergy analysis with multi-objective analysis for a trigeneration system consisting of a gas turbine cycle absorption

system and ORC using R600a and R141b as ORC working fluid. After optimisation, the system presented the highest energy and exergy efficiency of 80.55 % and 41.89 %, respectively; using an R600a leads to cost reduction more than 12 times that of R245fa.

According to the state-of-the-art review, it is evident that there is a great deal of interest in ORC-VCC trigeneration. However, the development of ORC-VCC systems powered by ground source energy and VCC improved through heat exchangers, and ejectors still face proven research gaps. Previous trigeneration studies have yet to be conducted on all proposed configurations. The work aims to delve into three different arrangements of combined ORC and compound ejector VCC (VCE) from energy and exergy perspectives.

The novel system arrangements gathered two promising techniques that contribute to overall system performance ameliorate: VCE condenser waste heat recuperation (more heat added to ORC, more generated power) and ejector-compressor combination (leads to compressor consumption power reduction so as enhance VCE COP). An associated renewable energy source that is a ground source heat source utilised for power generation is used the surplus ground source water from the ORC evaporator to satisfy the building and greenhouse heating demand. Moreover, two chilled water evaporators of different supply temperature levels are obtained to meet the building's cooling demand and greenhouse.

In the power-cooling mode, the heat pump condenser waste heat is employed to enhance the ORC power generation at low-grade ground source heat temperature. In the power-heat pump heating mode, the heat pump utilised all ORC condenser waste heat and upgraded this heat to beneficial temperature levels (60 ℃, typical district heating delivered temperature), which is actuated when the ground source temperatures are less than 65 ℃. The final mode is the power-ground source heating mode, where the surplus ground source waste heat from the ORC evaporator is used directly for heating purposes. R1234ze(E), R1234yf, and R1243zf are working refrigerants.

This work proposed several compound system configurations that generate power, cooling, and heating. This work is mainly concerned with the proposal of several novels combined ORC-compound ejector-VCC system (ORVCE) configurations for three purposes: power-cooling, power-heat pump heating, and power-ground source heating, with a higher overall system COP under different conditions. Ultra-low GWP refrigerants and condenser waste heat utilisation were proposed, and the system feasibility under different conditions and comparing energy and exergy with covenantal ORC and VCC systems was evaluated. The simulation analyses are established by Engineering Equation Solver (EES) software.

2. System description

2.1. Configurations

The new arrangement consists of an ORC combined with a compound greenhouse waste heat-driven ejector-VCC for energy-efficient power-cooling and heating purposes. The system operates in a wide range of ground source temperatures with moderate to low energy consumption and high power generation. The system can utilise heat sources for power generation in three modes: power-cooling, power-heat pump heating, or power-ground source heating modes.

This system uses waste heat from two different sources for multi-purpose simultaneous cooling, heating, and power generation, with an associated ground source that supports the ORC. System configurations align with the International Energy Agency's vision of the 2050 technology roadmap, which recommends designing systems for simultaneous heating, cooling, and power production.

The power-cooling mode system components are shown in (Fig. 1.a). In this arrangement, ORC and VCE are coupled by a flash tank intercooler. The system uses heat from a ground source to produce power and cooling at two levels (residential air conditioning and greenhouse cooling). The condenser waste heat increases the ORC performance, while greenhouse waste heat is used as the evaporator heat source. The vapour generated in an evaporative-condenser is the ejector driving force (removing the ejector pump). The VCE operates with lower consumption power and higher COP than traditional VCC. This configuration is proposed when there is no heating demand.

The refrigerant undergoes several thermodynamic processes in the power-cooling mode, explained in the following. Firstly, superheated refrigerant is expanded in the turbine to the condenser pressure (state 17). Then, in the low-temperature recapture, it exchanges heat with the second stream (10). Constant pressure heat rejection occurs at the first condenser (10′), where the refrigerant is in a two-phase state. The refrigerant is divided into two streams; one passes to the second condenser, which is wholly condensed and exits as saturated liquid (11). The other goes to the separation tank, where an adiabatic separation occurs and leaves liquid refrigerant from the bottom (5) and saturated vapour from the upper side (4). The first one undergoes throttling at the first expansion valve (5′). Heat exchange takes place between saturated vapour (4) and mixture refrigerant (5′) at the evaporative-condenser and becomes saturated liquid (8). Next, it absorbs heat from the building in the low-temperature evaporator and fully converts it to superheated vapour (9). On the other side, after exchanging heat in the evaporative-condenser, the two-phase refrigerant absorbs heat from the greenhouse (7). A mixing process occurs in the ejector and exits at suction compressor pressure (1), where it is suctioned and compressed to condenser pressure (2), exchanging heat in the high-temperature recapture heat exchanger. After exchanging heat at the high-temperature recapture (2), it undergoes a direct contact cooling process with the saturated liquid stream at the intercooler tank (11). The saturated liquid refrigerant is pumped to turbine pressure by the ORC pump (13). Then, it is separated into two streams, one exchanging heat in the low-temperature recapture (14′) while the other exchanges heat in the high-temperature recapture (14). The two streams are again mixed (15). The heat exchange in the ORC evaporator with ground source water takes place and becomes superheated refrigerant (16), and finally, it is delivered to the turbine.

In the power-heat pump heating mode (Fig. 1.b), the system includes all ORC components (without the condenser) and a VCC compressor, condenser, back-pressure valve (reducing the heat pump condenser pressure to the flash tank pressure), and flash intercooler tank. The heat pump uses all ORC waste heat by direct contact flash intercooler tank and increases it to district heating temperatures. The surplus heat from the water leaving the ORC evaporator is utilised for greenhouse heating instead of being rejected to the well. This Modified Organic-Vapour Compression system (MORVC) mode is actuated when the ground source temperatures are below 65℃. This arrangement can operate with the lowest ground source temperature and highest performance.

Again, the refrigerant undergoes the processes described in the following: Superheated refrigerant expansion in the turbine to a condenser pressure (leaving at state 8). Then it passes through the low-temperature recapture, which exchanges heat with the second stream (9). The flash tank is fed, and the refrigerant undergoes a constant pressure direct contact cooling process with the stream exiting the condenser. Next, after a separation process, liquid refrigerant is taken from the bottom of the tank (4) and saturated vapour from the upper part (1). The ORC pumps the liquid refrigerant to the highest pressure in the cycle (5). It passes through the low-temperature recapture and exchanges heat with the expanded refrigerant exiting the turbine (6). It undergoes constant heat exchange with ground source water and becomes superheated (7). The saturated vapour from the flash tank's upper side is compressed to condenser pressure, exchanges heat with the building, and condenses to a saturated liquid (3). Finally, it undergoes a throttling process by the back-pressure valve to the flash intercooler pressure (3‘), and direct contact cooling takes place at the flash intercooler.

In the power-ground source heating mode, the system comprises only

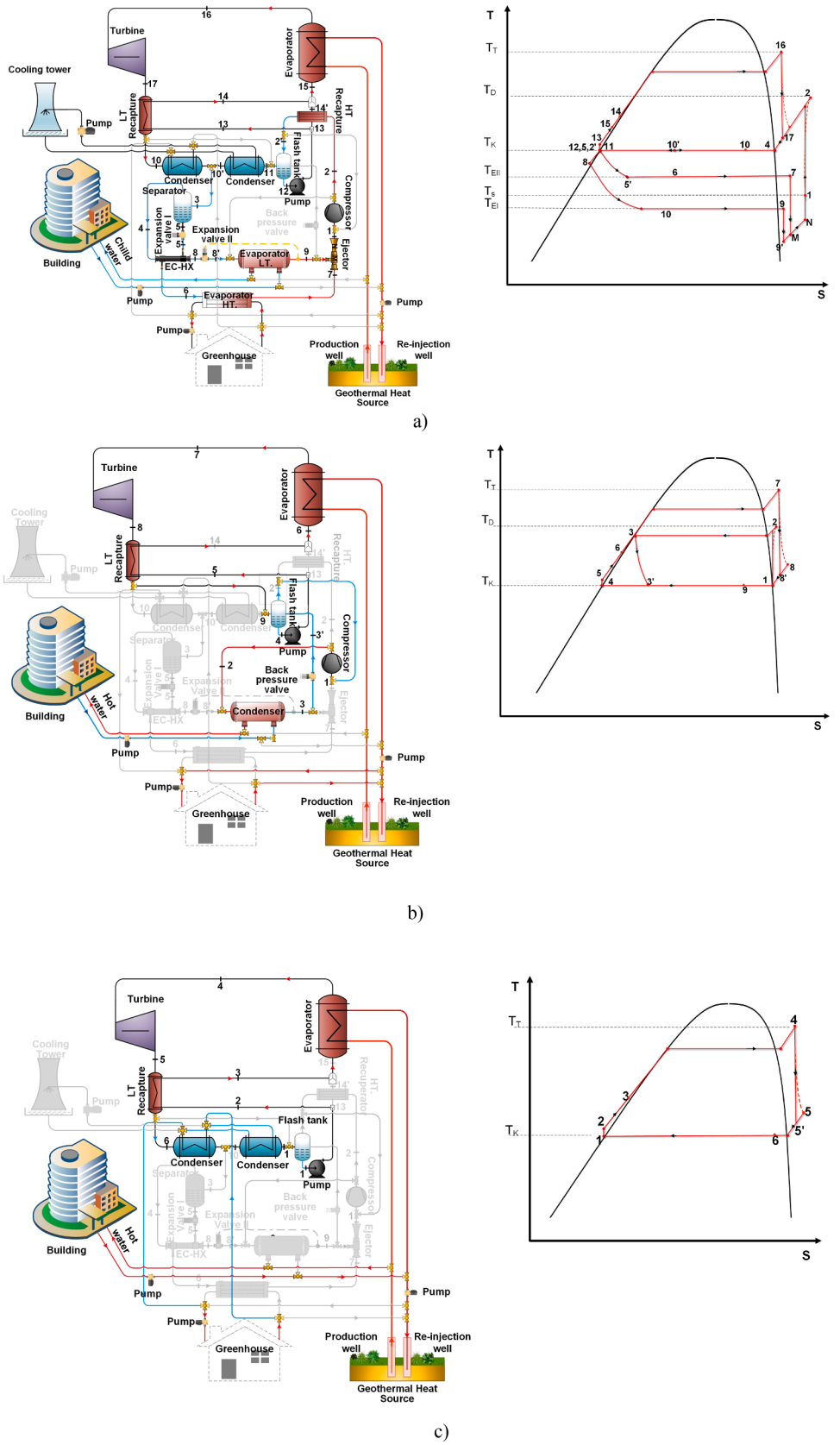

Fig. 1. Schematic and P-h diagram of the studied system, modes: a) power-cooling (ORVCE), b) power-heat pump heating (MORVC), and c) power-ground source heating.

Table 1
Important properties of studied refrigerants [48 49].

Refrigerants	Molecular weight (g mol^{-1})	T_{crit} (°C)	P_{crit} (bar)	NBP (°C)	ρ_{v} (kg m^{-3})	h_{fg} (kJ kg^{-1})	ODP	GWP_{100}	Safety class ASHRAE
R1234ze(E)	114.0	109.4	36.32	–19.28	5.71	195.6	0	7	A2L
R1234yf	114.0	94.7	33.82	–29.49	5.98	180.2	0	4	A2L
R1243zf	96.1	103.8	35.18	–25.43	4.95	217.2	0	1	A2L

*At a pressure of 1.01325 bar.

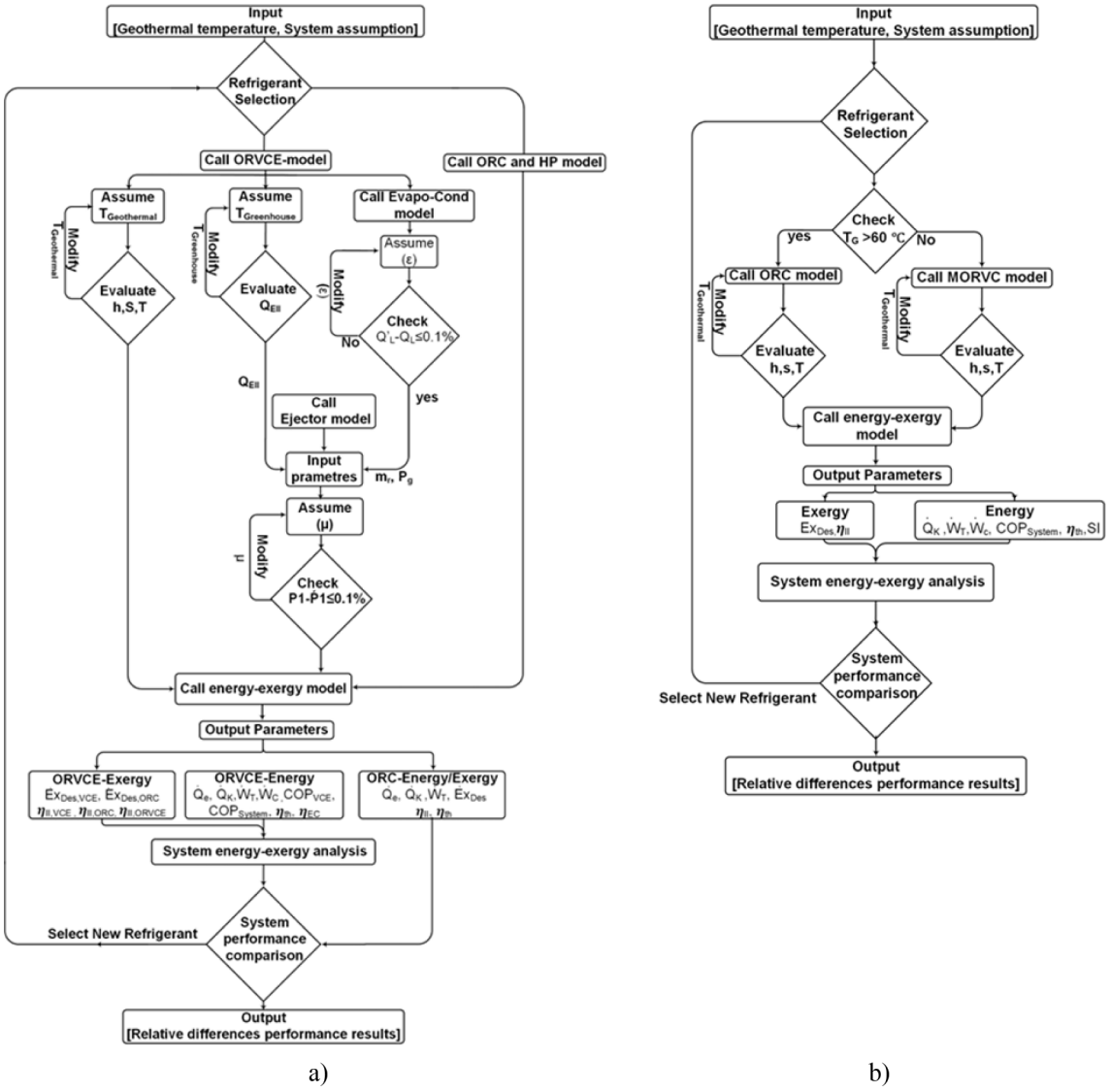

Fig. 2. Modelling flow chart: a) power-cooling and b) power-heating modes.

ORC components (Fig. 1.c), which is actuated at higher ground source temperatures (more than 65 °C). The system uses surplus ground source waste heat from the ORC evaporator outlet directly for heating, which is more efficient than increasing ORC condensing temperature (a higher condensing temperature results in lower ORC performance, power production, and thermal efficiency). In this configuration, the condenser waste heat is utilised for greenhouse heating purposes rather than released into the surrounding air (in the absence of a cooling tower). For this reason, flash tanks eliminate gas bubbles flowing into pump suction (preventing pump cavitation in case of incomplete condensation).

2.2. *Working fluids*

Assessing the proposed system in-depth is essential to determine the most suitable alternative refrigerant. The current study considers three ozone-friendly and ultra-low GWP (lower than 10) refrigerants, R1234ze(E), R1243zf, and R1234yf, which present comparable performance in previous studies [47]. Table 1 shows the important properties of the studied refrigerants. Only minor differences will likely impact the operating parameters and system efficiency.

3. Methodology

3.1. System modelling

The Engineering Equation Solver (EES) software [48] is used in system modelling, including the built-in thermodynamic properties of different refrigerants, the proposed system models, and all assumptions, boundary conditions, and inputs. Moreover, the model also considers different configurations, the influence of ground source temperatures, ORC, and heat pump ejector sub-models, among others. Fig. 2 presents the methodology flow chart for the different modes of the ORVCE.

3.2. Simulation method and conditions

To present a sensitive energy and exergy performance analysis, the ground source temperatures, condensing temperature, and greenhouse inlet temperature are varied individually with constant evaporator building load and temperature (low-temperature evaporator). An ideal flash tank intercooler is considered a saturated liquid from where the refrigerant leaves. The flow and heat losses in pipes and connections are abandoned. All boundary conditions and assumptions used in system modelling are summarised in Table 2.

3.3. Mathematical models

3.3.1. Energy model

The energy mathematical model for each system component is summarised in Table 3. More details about the ejector model used in the current study are mentioned and validated by Al-Sayyab et al. [47].

Sub-system ORC and VCE performances are combined to determine the overall system performance. The VCE energy performance in cooling and heating modes is determined by the COP, which can be calculated through Eq. (1) and (2), respectively.

$$COP_C = \frac{\dot{Q}_e}{\dot{W}_C} \tag{1}$$

$$COP_H = \frac{\dot{Q}_K}{\dot{W}_C} \tag{2}$$

The ORC's thermal efficiency can be obtained by Eq. (3).

$$\eta_{th} = \frac{\dot{W}_{net}}{\dot{Q}_{in}} \tag{3}$$

In the power-cooling mode, Eq. (4) and (5) are used, whereas, in power-heating modes, Eq. (6) and (7).

$$\dot{W}_{net} = \dot{W}_T - \dot{W}_P - \dot{W}_C \tag{4}$$

$$\dot{Q}_{in} = \dot{Q}_{e,ORC} + \dot{Q}_{R,LT} \tag{5}$$

$$\dot{W}_{net} = \dot{W}_T - \dot{W}_P \tag{6}$$

$$\dot{Q}_{in} = \dot{Q}_{e,ORC} \tag{7}$$

Finally, by using Eq. (8), the overall system performance can be evaluated as follows:

$$COP_{System} = COP\eta_{th} \tag{8}$$

3.3.2. Exergy model

The irreversibility source and magnitude are crucial to increasing and optimising system performance. The exergy analysis indicates the inefficient part of the thermal system. Ambient conditions are taken as the reference state. The nominal exergy balance equation can be written as indicated in Eq. (9) and (10) [56].

$$0 = \left(1 - \frac{T_0}{T_b}\right) Q - \dot{W} + \dot{E}x_{in} - \dot{E}x_{out} - \dot{E}x_{Des} \tag{9}$$

$$\dot{E}x = \dot{m}(h - h_0 - T_0(s - s_0)) \tag{10}$$

The exergy destruction mathematical models of each ORVCE component are summarised in Table 4.

Also, the heat pump total exergy destruction rate is obtained by Eq. (11).

Table 2
Assumptions and boundary conditions.

Parameters	Assumed value
$T_{K,ORVCE}$	27 to 35 °C
$T_{LT,e}$	2 °C
$\Delta T_{cooling\ media}$	5 °C
$T_{K,heat\ pump}$	60 °C
Cooling capacity	120 kW
$T_{greenhouse}$	28 to 38 °C
T_G	55 to 90 °C [50]
$\dot{m}_G$	7.5 kg s^{-1} [51]
$\dot{m}_r$	11 kg s^{-1}
η_{np}	0.90 [52]
η_{ns}	95 %[53]
η_D, η_{mx}	85 % [47]
ε_{HX}	80 % [22]
η_{em}	88 % [54]
$\eta_{is,t}$	80 % [55]

Table 3
Energy and mass balance equations for ORVCE components.

Components	Energy balance equations		Mass balance
	Power-cooling mode	Power-heating modes	
Pump	$\dot{W}_P = \dot{m}_r(h_{13} - h_{12})$	$\dot{W}_P = \dot{m}_r(h_5 - h_4)$	N/A
LT Recapture	$\dot{Q}_{R,LT} = \dot{m}_{13}(h_{14'} - h_{13}) = \dot{m}_1(h_2 - h_{2'})$	N/A	N/A
HT Recapture	$\dot{Q}_{R,HT} = \dot{m}_r(h_{17} - h_{10}) = \dot{m}_{14}(h_{14} - h_{13})$	$\dot{Q}_{R,HT} = \dot{m}_r(h_8 - h_9) = \dot{m}_r(h_6 - h_5)$	N/A
Mixing tank	$\dot{m}_r h_5 = \dot{m}_{13} h_{14} + \dot{m}_{14} h_{14'}$	N/A	$\dot{m}_r = \dot{m}_{13} + \dot{m}_{14}$
ORC evaporator	$\dot{Q}_{e,ORC} = \dot{m}_r(h_{16} - h_{15}) = \dot{m}_G(h_{in} - h_{out})$	$\dot{Q}_{e,ORC} = \dot{m}_r(h_7 - h_6) = \dot{m}_G(h_{in} - h_{out})$	N/A
Turbine	$\dot{W}_T = \dot{m}_r(h_{16} - h_{17})$	$\dot{W}_T = \dot{m}_r(h_7 - h_8)$	N/A
ORC condenser	$\dot{Q}_{K,ORC} = \dot{m}_r(h_{10} - h_{11})$		N/A
Flash tank	$\dot{m}_r h_{12} = \dot{m}_{11} h_{11} + \dot{m}_1 h_{2'}$	$\dot{m}_r h_{12} + \dot{m}_1 h_1 = \dot{m}_r h_9 + \dot{m}_1 h_{3'}$	$\dot{m}_r = \dot{m}_{11} + \dot{m}_1$
Compressor	$\dot{W}_C = \dot{m}_1(h_2 - h_1)$	$\dot{W}_C = \dot{m}_1(h_2 - h_1)$	N/A
LT Evaporator	$\dot{Q}_{e,LT} = \dot{m}_5(h_7 - h_6)$	N/A	N/A
HT Evaporator	$\dot{Q}_{e,HT} = \dot{m}_4(h_9 - h_8)$	N/A	N/A
Separator	$\dot{m}_1 h_3 = \dot{m}_4 h_4 + \dot{m}_5 h_5$	N/A	$\dot{m}_1 = \dot{m}_4 + \dot{m}_5$
Condenser	N/A	$\dot{Q}_K = \dot{m}_1(h_2 - h_3)$	N/A

N/A: Not applicable

Table 4
Exergy destruction rate mathematical models for ORVCE components [56,59,60].

Component	Equation
Pump	$\dot{E}x_{Des,P} = \dot{E}x_{in} - \dot{E}x_{out} + \dot{W}_P$
LT recapture	$\dot{E}x_{Des,R,LT} = (\dot{E}x_{in} - \dot{E}x_{out})_{r,ORC} + (\dot{E}x_{in} - \dot{E}x_{out})_{r,VCE}$
HT recapture	$\dot{E}x_{Des,R,HT} = (\dot{E}x_{in} - \dot{E}x_{out})_{rl} + (\dot{E}x_{in} - \dot{E}x_{out})_{rh}$
Mixing	$\dot{E}x_{Des,M} = \dot{E}x_{in} - \dot{E}x_{out}$
ORC evaporator	$\dot{E}x_{Des,e,ORC} = (\dot{E}x_{in} - \dot{E}x_{out})_r + (\dot{E}x_{in} - \dot{E}x_{out})_G$
Turbine	$\dot{E}x_{Des,T} = \dot{E}x_{in} - \dot{E}x_{out} - \dot{w}_T$
ORC condenser	$\dot{E}x_{Des,K,ORC} = (\dot{E}x_{in} - \dot{E}x_{out})_r + (\dot{E}x_{in} - \dot{E}x_{out})_w$
Flash tank intercooler	$\dot{E}x_{Des,FT} = \dot{E}x_{in} - \dot{E}x_{out}$
Compressor	$\dot{E}x_{Des,C} = \dot{E}x_{in} - \dot{E}x_{out} + W_C$
Condenser	$\dot{E}x_{Des,K} = (\dot{E}x_{in} - \dot{E}x_{out})_r + (\dot{E}x_{in} - \dot{E}x_{out})_w$
Evaporative-Condenser	$\dot{E}x_{Des,ek} = (\dot{E}x_{in} - \dot{E}x_{out})_{rl} + (\dot{E}x_{in} - \dot{E}x_{out})_{rh}$
HT evaporator	$\dot{E}x_{Des,e,HT} = (\dot{E}x_{in} - \dot{E}x_{out})_r + (\dot{E}x_{in} - \dot{E}x_{out})_w$
Ejector	$\dot{E}x_{Des,ej} = \dot{E}x_{in} - \dot{E}x_{out}$
Expansion valve	$\dot{E}x_{Des,exp} = \dot{E}x_{in} - \dot{E}x_{out}$
LT evaporator	$\dot{E}x_{Des,e,LT} = (\dot{E}x_{in} - \dot{E}x_{out})_r + (\dot{E}x_{in} - \dot{E}x_{out})_w$

$$\dot{E}x_{Des,VCE} = \dot{E}x_{Des,C} + \dot{E}x_{Des,K} + \dot{E}x_{Des,LT,e} + \dot{E}x_{Des,ej} + \dot{E}x_{Des,exp} + \dot{E}x_{Des,HT,e} \tag{11}$$

The second law efficiency of the VCE is obtained by Eq. (12).

$$\eta_{II,VCE} = 1 - \frac{\dot{E}x_{Des,VCE}}{\dot{E}x_{in}} \tag{12}$$

Likewise, the ORC total exergy destruction rate is obtained by Eq. (13).

$$\dot{E}x_{Des,ORC} = \dot{E}x_{Des,T} + \dot{E}x_{Des,K,} + \dot{E}x_{Des,e,} + \dot{E}x_{Des,P} + \dot{E}x_{Des,R(HT,LT)} + \dot{E}x_{Des,M} + \dot{E}X_{Des,FT} \tag{13}$$

The ORC exergy efficiency is determined by Eq. (14).

$$\eta_{II,ORC} = 1 - \frac{\dot{E}x_{Des,ORC}}{\dot{E}x_{in}} \tag{14}$$

Finally, the overall ORVCE exergy efficiency can be evaluated, as shown in Eq. (15).

$$\eta_{II,system} = \eta_{II,VCE}\eta_{II,ORC} \tag{15}$$

Besides optimising the efficiency of any energy conversion system, the environmental impact should also be considered. The sustainability index (SI) is obtained by Eq. (16), linking exergy and environmental effect [57].

$$SI = \left(\frac{\dot{E}x_{Des}}{\dot{E}x_{in}}\right) \tag{16}$$

The system's economic efficiency can be calculated in power-cooling mode by Eq. (17) and in power-heating mode by Eq. (18) [58].

$$\eta_{EC} = \frac{\dot{W}_{net} + 0.8\dot{Q}_{e,VCE}}{\dot{Q}_{e,ORC}} \tag{17}$$

$$\eta_{EC} = \frac{\dot{W}_{net} + 0.5\dot{Q}_{K,ORC}}{\dot{Q}_{e,ORC}} \tag{18}$$

4. Results and discussion

4.1. Power-cooling mode

4.1.1. Low GWP refrigerant selection

This work considers three environmentally-friendly (ultra-low GWP) refrigerants, R1234ze(E), R1243zf, and R1234yf (main characteristics in Table 1).

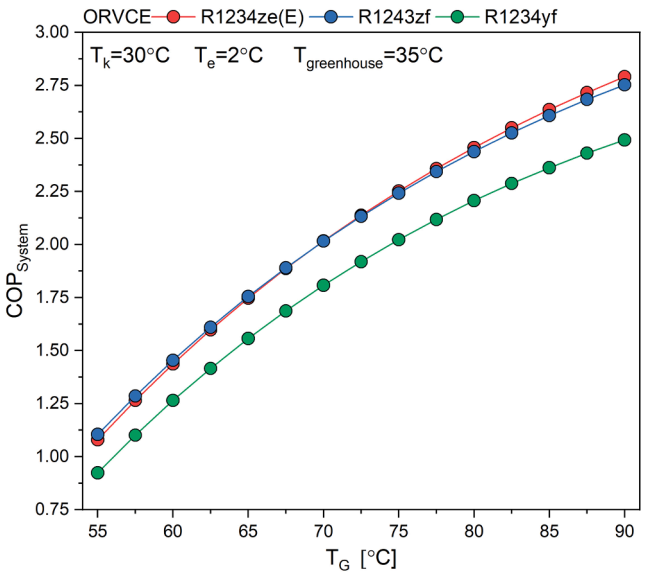

Fig. 3. System COP at different ground source temperatures for R1234ze(E), R1243zf, and R1234yf.

The average overall COP is a figure of merit in selecting a suitable refrigerant with efficient ORVCE thermal efficiency. Fig. 3 shows that R1234ze(E) delivers the highest COP_{System} at higher ground source temperatures and is slightly lower than R1243zf at ground source temperatures below 65 °C. Regarding the average value of the COP_{System}, R1234ze(E) shows the highest value. Consequently, it is selected as the ORVCE working refrigerant for sensitivity analyses.

4.1.2. Influence of ground source temperatures variation on system performance

Fig. 4.a shows the ORC evaporator capacity at different ground source temperatures in the power-cooling mode. The ground source temperatures increase ORC evaporator capacity and power generation. In the same way, at a given ground source temperature, a higher condensing temperature (and pressure) decreases the turbine power generation because of a volume ratio reduction (turbine expansion ratio decrement).

While increasing ground source temperatures does not influence VCE COP, Fig. 4.b, a higher condensing temperature increments compressor power consumption (following pressure ratio increase, Fig. 4.c). Moreover, the refrigerant mass flow rate is also increased, Fig. 4.d (refrigerant density increases at turbine suction, despite volumetric efficiency reduction, Fig. 4.e). Consequently, thermal efficiency increases (Fig. 4.f) due to generated power augmentation at a given compressor pressure ratio and pump operating power. In contrast, the condenser temperature increase has a reducing influence on both net generated power and thermal efficiency owing to the rise in compressor consumption (higher compressor pressure ratio) associated with the decrease in the turbine power generation (lowest turbine expansion ratio).

Fig. 5 shows the effect of ground source temperatures on evaporator capacity at different condensing temperatures. The highest evaporator capacity and power generation are obtained at a condenser temperature of 27 °C due to a refrigerant density increase at the turbine inlet associated with the highest turbine expansion ratio.

Fig. 6.a shows that the ground source temperature increase positively influences system COP; ORVCE performance follows ORC behaviour with ground source temperatures. Power generation and thermal efficiency are directly proportional to ground source temperatures Fig. 4.f. On the other hand, the condensing temperature increase

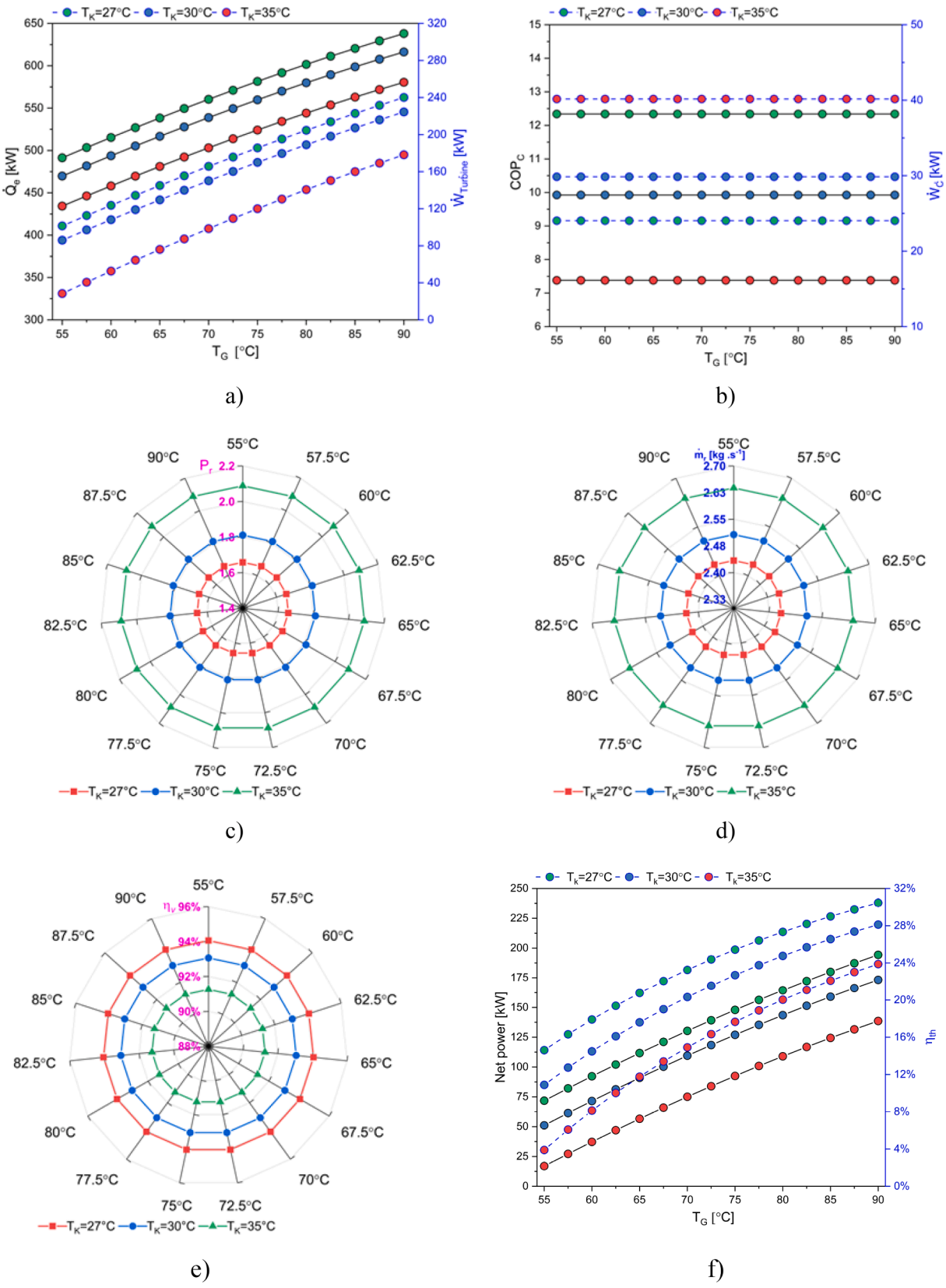

Fig. 4. Influence of ground source temperature variation on a) power generation and evaporator capacity, b) cop and power consumption, c) pressure ratio, d) mass flow rate, e) volumetric efficiency, and f) net power and thermal efficiency. for blue contour symbols and lines, please refer to the right axis. (For interpretation of the references to colour in this figure legend, the reader is referred to the web version of this article.)

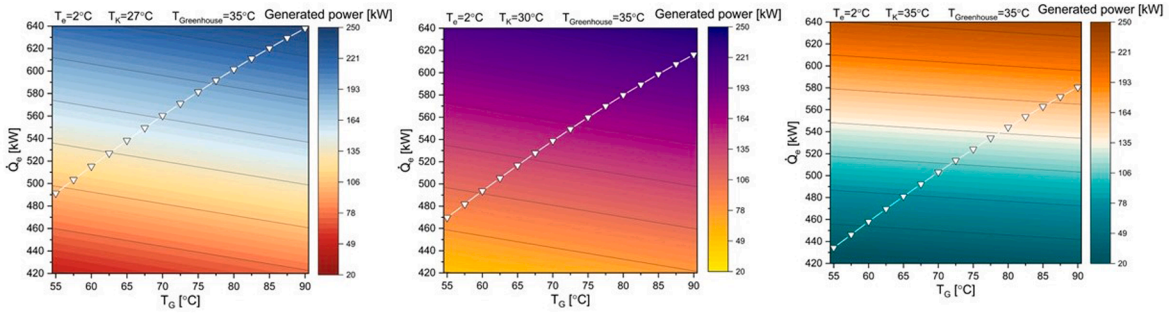

Fig. 5. Effect of ground source temperatures on power generation and evaporator capacity at different condensing temperatures.

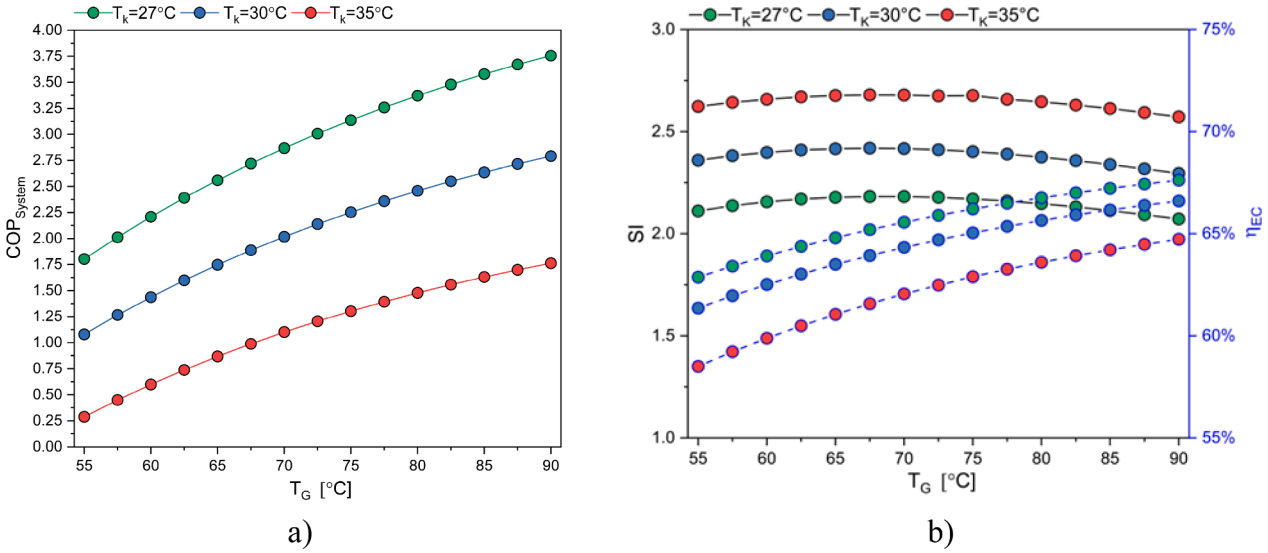

Fig. 6. Influence of ground source and condensing temperature variation on: a) system COP, and b) SI and economic efficiency. For blue contour symbols and lines, please refer to the right axis. (For interpretation of the references to colour in this figure legend, the reader is referred to the web version of this article.)

has a reduced effect on the ORVCE performance at a given ground source temperature. It follows the ORC and VCE behaviour, a condensing temperature increase decrease the VCE COP_C, resulting from compressor power consumption increase, Fig. 4.b. The contrary occurs with power generation and thermal efficiency Fig. 4.f.

Besides, ground source temperature benefits thermal economic efficiency (Fig. 6.b) due to the net power generation increment. On the contrary, the SI slightly decreases owing to the exergy destruction increase (Fig. 6.b), owing to the higher temperature differences across the evaporator.

4.1.3. *Effect of greenhouse temperature*

Fig. 7 shows the effect of greenhouse temperature on system performance for given condensing and ground source temperatures. The current system utilises the greenhouse waste heat as the ejector driving force. Due to ejector pressure increase, a higher greenhouse temperature reduces compressor power consumption (and pressure ratio, Fig. 7.a). Additionally, the refrigerant mass flow rate decreases with the greenhouse temperature increase due to the cooling load requirement reduction with superheating degree increment.

Similarly, the greenhouse temperature slightly affects the ORVCE net power generation for ground source supply and condenser temperatures. In contrast, it modestly increases the thermal efficiency, associated with an increase in the overall system COP (Fig. 7.c). This phenomenon can be explained by the increase in the VCE COP caused by the compressor power consumption reduction (Fig. 7.b).

Finally, the greenhouse temperature has a minor influence on economic efficiency and SI due to a slight effect on power consumption and irreversibilities.

4.1.4. *Exergy analysis*

This section analyses the ORVCE exergy performance at different ground source and fixed condensing and evaporating temperatures. Fig. 8 states that the low-temperature recapture heat exchanger represents the largest source of exergy destruction in the whole system, followed by the turbine and high-temperature recapture heat exchanger (47 %, 25 % and 11 %, respectively). On the other hand, the contribution of the evaporative-condenser and the first expansion valve to the exergy destruction is considered negligible.

Fig. 9.a states that the ground source temperatures do not affect VCE exergy destruction and efficiency. Moreover, higher condenser temperatures decrease the ejector-heat pump exergy performance because the compressor exergy destruction follows the pressure ratio increase.

Besides, the ORC exergy efficiency benefits from a higher ground source temperature (Fig. 9.b), attending to lower total exergy destruction than the total exergy input. In the same way, the condensing temperature lessens the ORC exergy performance because of a higher temperature difference across the evaporator and condenser and a lower turbine expansion ratio. In light of the above result, the ORVCE exergy performance has the same behaviour as the sub-cycles (ORC and VCE). This increases at higher ground source temperatures, Fig. 9.c. On the other hand, at a condensing temperature of 27 °C, the highest ORVCE exergy efficiency is observed due to less exergy destruction for both turbine and compressor (higher turbine expansion ratio with lower

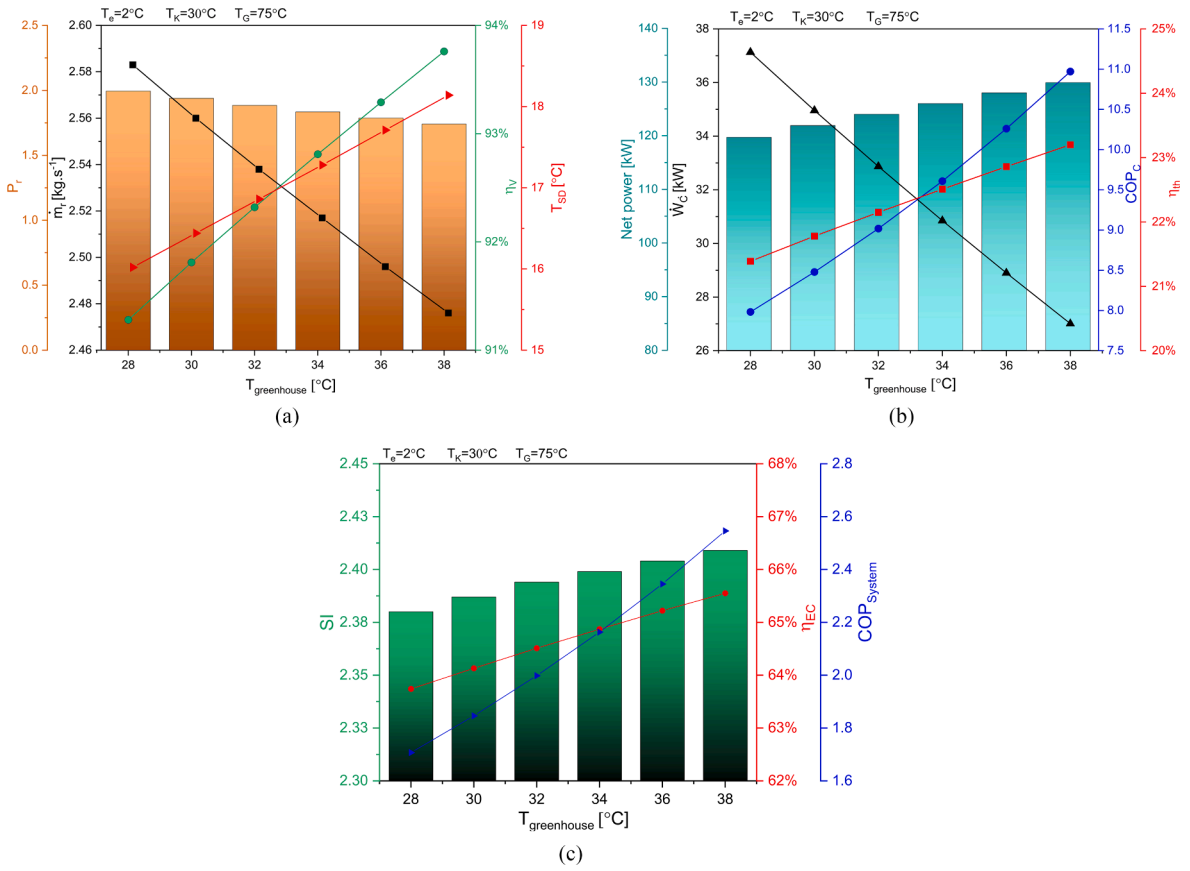

Fig. 7. Greenhouse temperature influence on a) refrigerant mass flow rate, b) power consumption, and c) SI and system COP. Please refer to the left axis for columns, whereas for lines and points, please refer to the right axis.

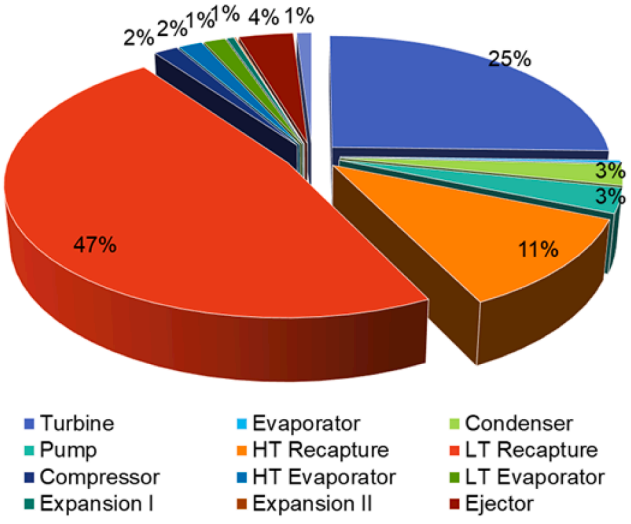

Fig. 8. ORVCE exergy destruction by component.

compressor pressure ratio).

Finally, a greenhouse temperature increase remarkably decreases the VCE exergy destruction (Fig. 10) due to the reduction in power consumption (Fig. 7.a) and temperature difference across the second evaporator and evaporative-condenser. As a result, the VCE exergy efficiency increased (Fig. 10). Moreover, the ORVCE exergy efficiency slightly increases due to the decrement in total exergy destruction (only VCE).

4.2. Power-heating mode

In this section, power-heating modes are presented. As mentioned, the power-heat pump heating mode (MORVC) is activated when the ground source temperature is below 65 ℃. On the other hand, the power-ground source heating mode is considered for ground source temperatures above 65 ℃. In this case, the system uses the surplus ground source heat after exchanging it with the ORC evaporator for heating purposes.

Fig. 11.a shows that the ground source temperatures positively influence power generation and thermal efficiency. In the same context, when the ground source temperature is above 65 ℃, both power generation and thermal efficiency increase owing to the absence of the compressor power consumption.

Besides, the ground source temperatures favour the exergy efficiency, particularly above 65 ℃, due to the absence of the heat pump exergy destruction Fig. 11.b.

Finally, the power-ground source heating system arrangement shows a high thermal economic efficiency compared to the MORVC mode (Fig. 11.c) because of the condenser waste heat utilisation in greenhouse heating.

4.3. Comparison of novel system with simple ORC and heat pump

4.3.1. Power-cooling mode

This section considers power generation and thermal efficiency to compare the proposed system with a conventional ORC. As proved in previous sections, the ORVCE performs above the ORC single system in all evaluated ground source temperatures. Moreover, environmentally friendly alternatives decrease direct CO_2-eq emission due to lower GWP values than HFCs. Therefore, combining both sub-systems (ORC with

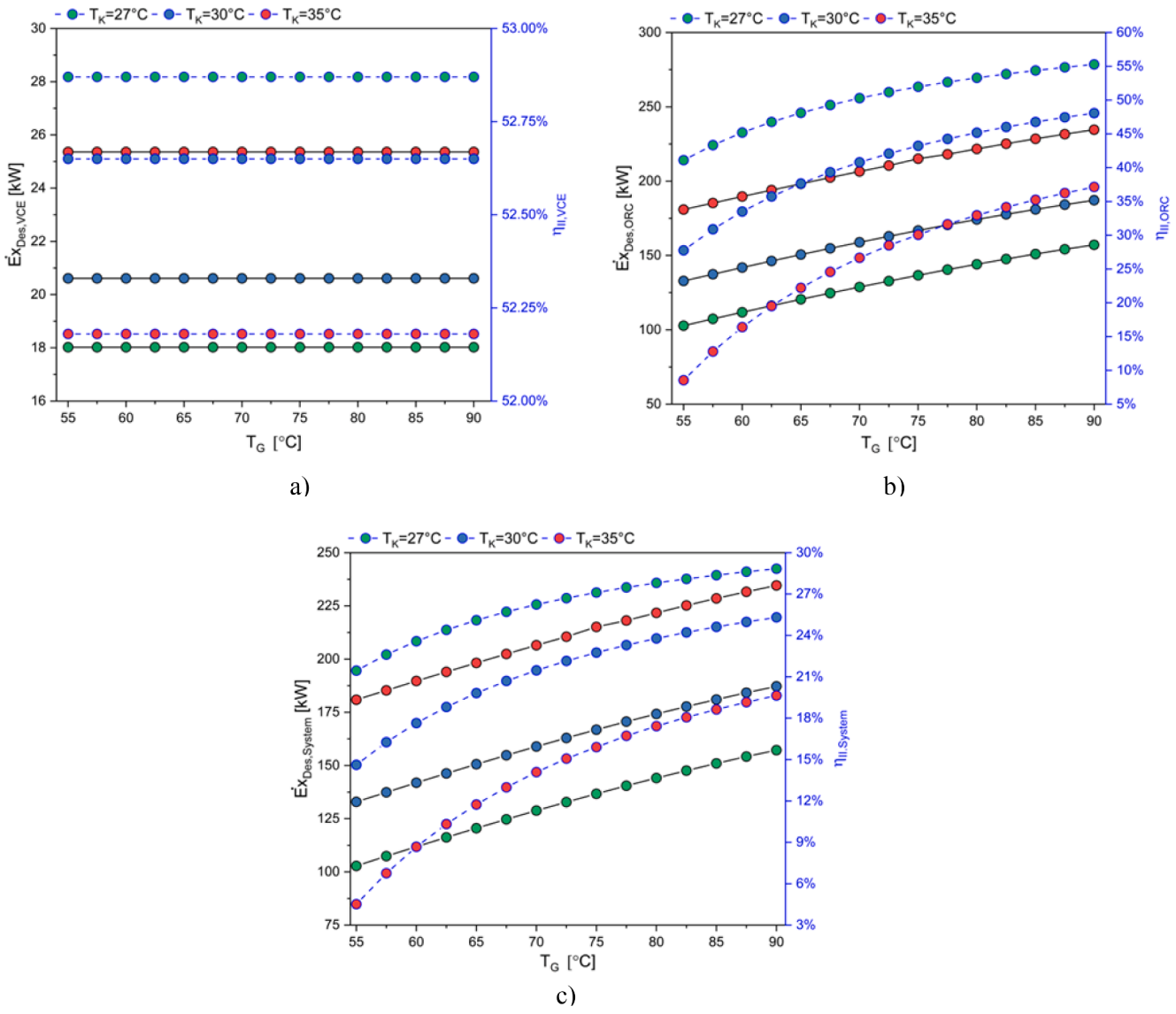

Fig. 9. Influence of ground source temperature on exergy performing of a) VCE, b) ORC economic, and c) ORVCE. For blue contour symbols and lines, please refer to the right axis. (For interpretation of the references to colour in this figure legend, the reader is referred to the web version of this article.)

VCE) results in significant carbon footprint reductions.

The ground source temperature increase has an enhancement influence on power generation. The proposed R1234ze(E) system obtained an average of 58 % higher power generation than a conventional ORC (Fig. 12.a), resulting in higher thermal efficiency, Fig. 12.b. Besides that, combining ORC with VCE increases the heat supplied to the ORC subsystem by utilising the VCE condenser waste heat.

4.3.2. Power-heating mode

This section considers the power generation to compare the combined system with a conventional ORC, considering the same heating capacity input.

The ORC uses half of the ground source heating capacity for power generation at low ground source temperatures, whereas the other half targets heating purposes, Fig. 13.a. The MORVC uses all ground source heating capacity for power generation with condenser waste heat utilisation as a heating source.

From Fig. 13.b, at low ground source temperatures (below 65 °C), the MORVC net power generation is always above ORC values. However, the MORVC system presents the highest thermal efficiency. The absence of heat pump power consumption benefits net power generation.

The heat pump operates at higher evaporator temperatures (ORC condensing temperature) than conventional units. Therefore, the current combination presents a higher heat pump COP due to a lower compressor power consumption than expected. Besides, the proposed system presents an economic benefit at low ground source temperatures.

5. System optimisation

Thermal analysis is nonlinear and depends on many thermal parameters due to the significant number of parameters involved in this complex system. After analysing the input parameters influence on the main operational and energy outputs, a multi-objective optimisation would benefit the overall COP to find the most efficient operating

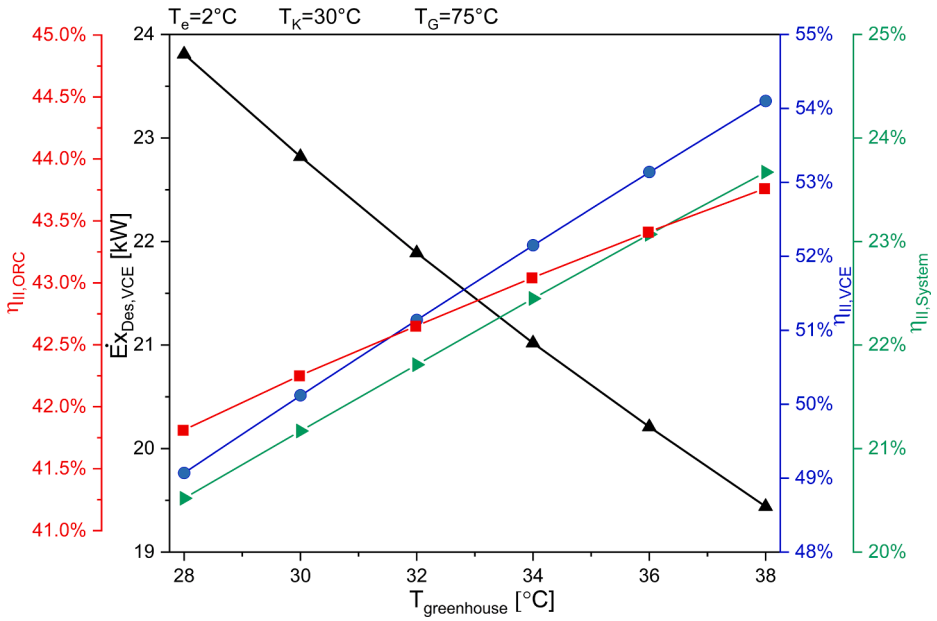

Fig. 10. System exergy performance variation over different greenhouse temperatures. Please refer to the right axis for blue and green contour symbols and lines. (For interpretation of the references to colour in this figure legend, the reader is referred to the web version of this article.)

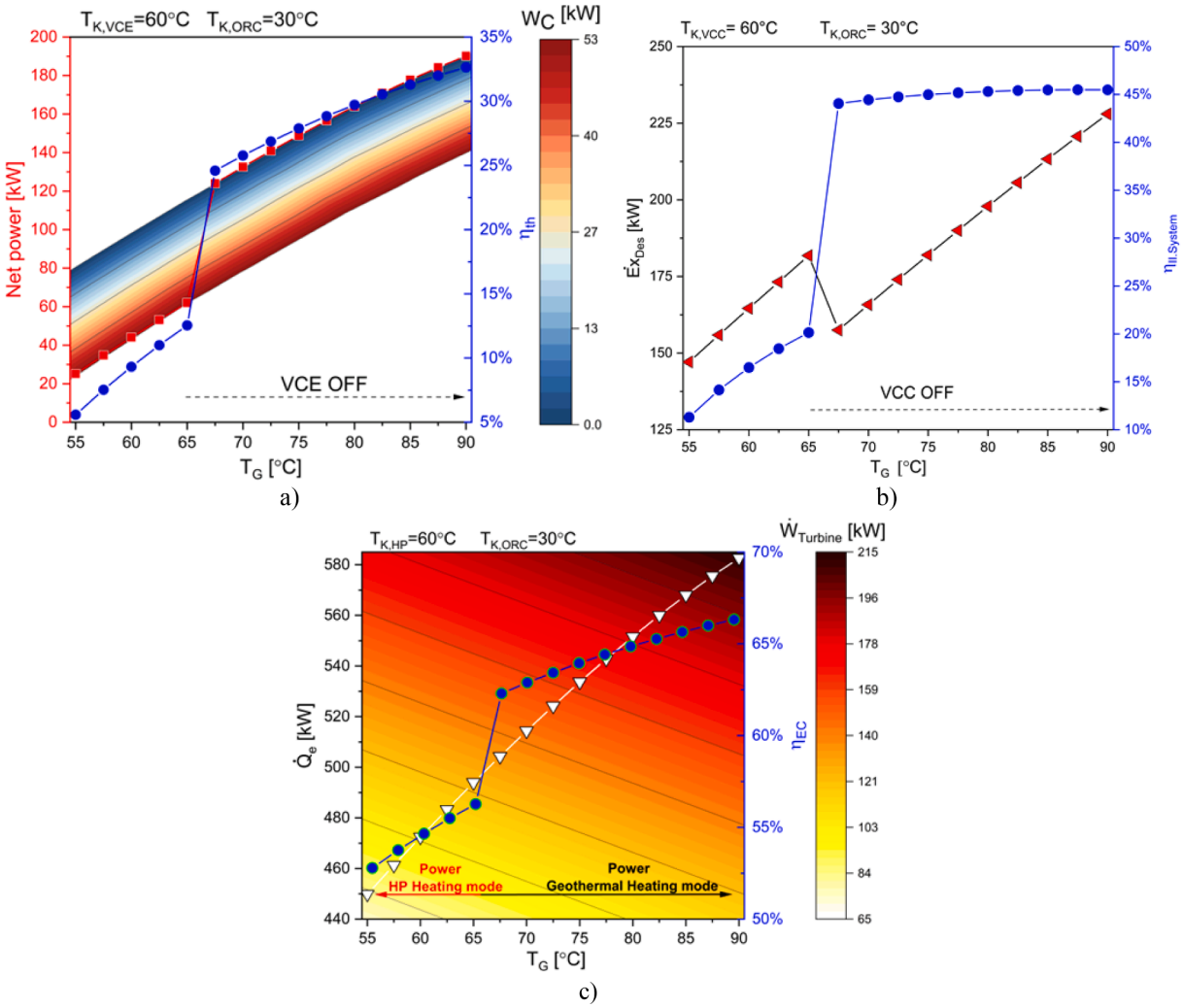

Fig. 11. Ground source temperature variation influence on a) net power generation, b) exergy destruction, and c) thermal economic efficiency. For blue contour symbols and lines, please refer to the right axis. (For interpretation of the references to colour in this figure legend, the reader is referred to the web version of this article.)

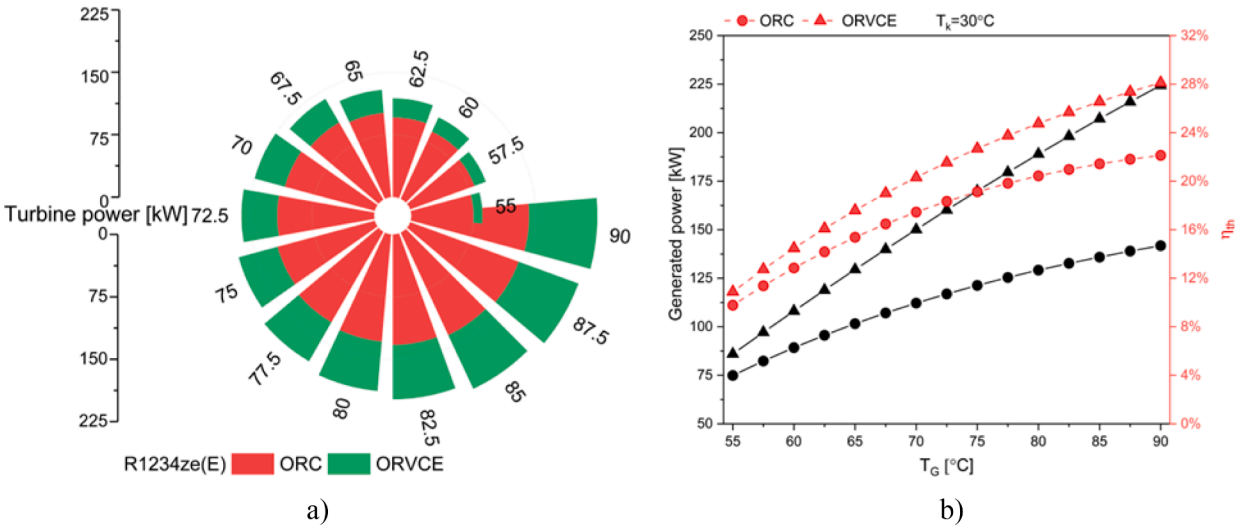

Fig. 12. ORVCE and ORC heat pump comparison under different ground source temperatures. For red contour symbols and lines, please refer to the right axis. (For interpretation of the references to colour in this figure legend, the reader is referred to the web version of this article.)

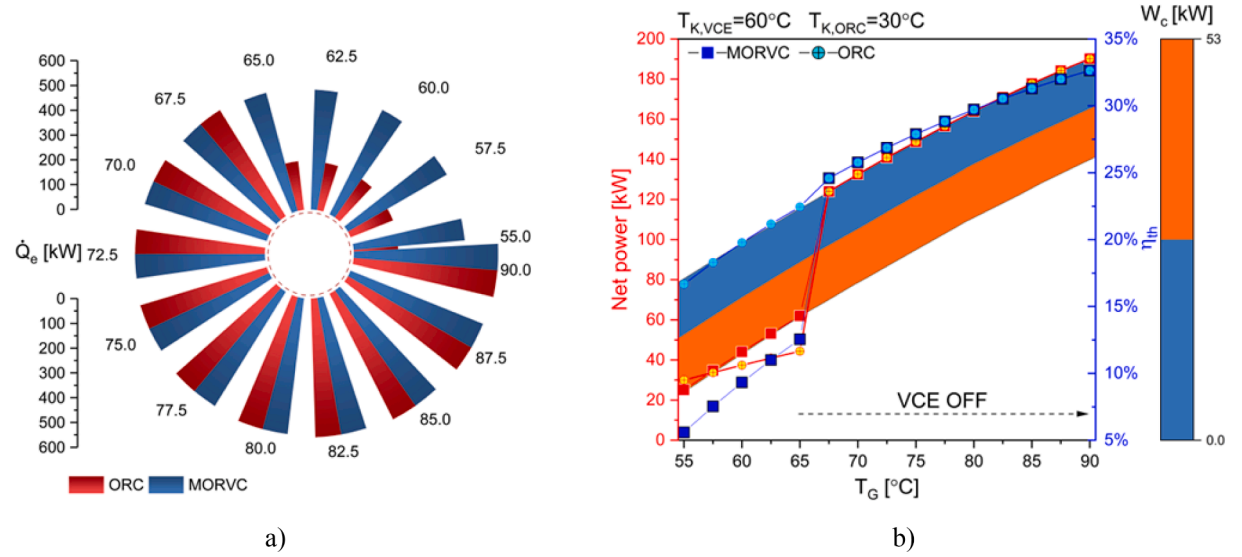

Fig. 13. MORVC and ORC comparison: a) Ground source heating capacity used and b) turbine net power generation. For blue contour symbols and lines, please refer to the right axis. (For interpretation of the references to colour in this figure legend, the reader is referred to the web version of this article.)

conditions for the ORVCE.

This section conducted an optimisation procedure using a professional version of EES. This version has steady-state multivariable optimisations methods, which minimise or maximises an objective function. A genetic algorithm was considered as the optimisation method. The objective function chosen was the maximisation of the system COP. Moreover, another parameter considering the total heat exchangers area per overall heat transfer coefficient divided by the net power consumption $\left(\frac{\sum UA}{\dot{W}_{net}}\right)$ [61] is minimised. This parameter is considered as an indicator of the installation costs. All required equations for evaluating the heat exchangers area and performance were taken from Al-Sayyab et al. [62]. The ranges of assessment variables for the optimisation are summarised in Table 5.

The optimised system performance was investigated over different geothermal supply temperatures, Fig. 14. The optimisation results increased system performance by 20 % to 28 % over the range of geothermal supply temperatures.

Table 5
Ranges of assessment variables for the system optimisation.

Independent input	Range	Optimum Value
$T_{greenhouse}$	15 to 25 ℃	25 ℃
T_K	27 to 38 ℃	27 ℃
ΔT_e	2 to 5 ℃	2 ℃
$\Delta T_{cooling\ media}$	5 to 15 ℃	9.5 ℃
ORC evaporator pinch point	5 to 15 ℃	7 ℃

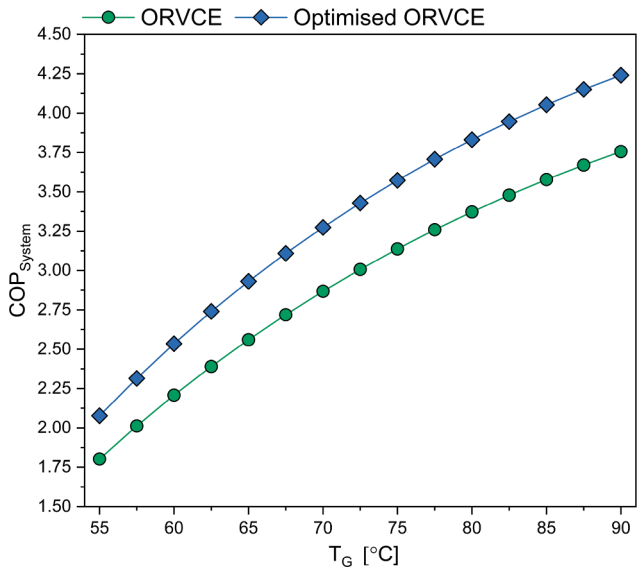

Fig. 14. Optimised system performance over different ranges of geothermal supply conditions.

6. Conclusions

This study presents an energetic and exergetic analysis of a novel arrangement of ORC and ejector-vapour compression combination for power–cooling and heating purposes with ground source and condenser waste heat revalorisation. The novel system arrangement is well-thought-out for three modes: power-cooling (two levels) with condenser waste heat utilisation, power-heat pump heating (for ground source temperatures below 65 ℃), and power-heating with ground source sources (for ground source temperatures above 65 ℃), including three ultra-low GWP refrigerants. The study conclusions are as follows.

- A higher ground source temperature increases power generation and overall system COP in all modes, if compared to conventional ORC and heat pump systems.
- The novel system arrangement using R1234ze(E) increases system COP by 18 % on average in the power-cooling mode. Besides, a low-temperature recapture heat exchanger for condenser waste heat recovery increases power generation by 58 %.
- Higher condensing temperatures decrease net power and system thermal efficiency. The optimum condensing temperature for any ground source temperature is 27 ℃.
- A higher greenhouse temperature increases the overall COP, with a modest increment in net power generation, thermal efficiency, economic efficiency and sustainable index. The last is justified because of the lower rise in power generation and irreversibility.
- Higher ground source temperatures for power-heating modes increase power generation and thermal efficiency. Compared to a conventional ORC, the MORVC presents the highest net power generation with an economic benefit at low ground source temperatures.
- The exergy efficiency follows the ground source temperatures for all modes. In the power-ground source heating mode, the exergy efficiency notably increased due to the absence of the heat pump exergy destruction.
- The optimisation results increased system performance by 20 % to 28 % over the range of geothermal supply temperatures.

This work has studied a novel combination of ORC and compound ejector-vapour compression to end with a highly energy-efficient thermodynamic system with ground source and condenser waste heat utilisation. Apart from the proposal assessed, this system could be coupled with other applications, such as absorption systems, which can utilise the condenser waste heat of ORC. Alternatively, two working fluids could be used to involve different operational conditions and modify the economic analysis. Finally, an exergoeconomic-exergoenvironmental analysis is an effective way to evaluate the proposed system components' benefits further and improve their efficiency.

CRediT authorship contribution statement

Ali Khalid Shaker Al-Sayyab: Conceptualization, Methodology, Software, Writing – original draft, Writing – review & editing. **Adrián Mota-Babiloni:** Conceptualization, Methodology, Writing – review & editing, Resources, Supervision. **Joaquín Navarro-Esbrí:** Writing – review & editing, Supervision, Project administration, Funding acquisition.

Declaration of Competing Interest

The authors declare that they have no known competing financial interests or personal relationships that could have appeared to influence the work reported in this paper.

Data availability

The authors are unable or have chosen not to specify which data has been used.

Acknowledgements

Ali Khalid Shaker Al-Sayyab gratefully acknowledges the Southern Technical University in Iraq for the financial support to complete this work. Adrián Mota-Babiloni acknowledges grant IJC2019-038997-I funded by MCIN/AEI/10.13039/501100011033.

References

[1] eurostar, Electricity production, consumption and market overview, (2021). https://ec.europa.eu/eurostat/statistics-explained/index.php?title=Electricity_production,_consumption_and_market_overview#Electricity_generation (accessed December 3, 2021).
[2] Matthias Buck, A. Graf, P. Graichen, A. Energiewende, European Energy Transition 2030: The Big Picture, Agora Energiewende. (2019). https://www.agora-energiewende.de/fileadmin/Projekte/2019/EU_Big_Picture/153_EU-Big-Pic_WEB.pdf.
[3] EPA, Global Greenhouse Gas Emissions Data, (2021). https://www.epa.gov/ghgemissions/global-greenhouse-gas-emissions-data (accessed December 3, 2021).
[4] Hartner M, Eeg TUW, Forthuber S, Eeg TUW, Müller A, Eeg TUW, et al. Electricity Demand From Heating and Cooling in Europe Until 2030. Heading Towards Sustainable Energy Systems: Evolution or Revolution? 2017.
[5] IEA, Net Zero by 2050: A Roadmap for the Global Energy Sector, International Energy Agency. (2021) 224.
[6] Lund JW. The USA geothermal country update. Geothermics 2003;32:409–18. https://doi.org/10.1016/S0375-6505(03)00053-1.
[7] Pierce V. Introduction to Geothermal power, first edit. The English Press; 2011.
[8] Li YM, Hung TC, Wu CJ, Su TY, Xi H, Wang CC. Experimental investigation of 3-kW organic Rankine cycle (ORC) system subject to heat source conditions: A new appraisal for assessment. Energy 2021;217:119342. https://doi.org/10.1016/j.energy.2020.119342.
[9] Quoilin S, Declaye S, Tchanche BF, Lemort V. Thermo-economic optimisation of waste heat recovery Organic Rankine Cycles. Appl Therm Eng 2011;31:2885–93. https://doi.org/https://doi.org/10.1016/j.applthermaleng.2011.05.014.
[10] Li J, Pei G, Ji J, Bai X, Li P, Xia L. Design of the ORC (organic Rankine cycle) condensation temperature with respect to the expander characteristics for domestic CHP (combined heat and power) applications. Energy 2014;77:579–90. https://doi.org/https://doi.org/10.1016/j.energy.2014.09.039.

[11] Meng N, Li T, Gao X, Liu Q, Li X, Gao H. Thermodynamic and techno-economic performance comparison of two-stage series organic Rankine cycle and organic Rankine flash cycle for geothermal power generation from hot dry rock. Appl Therm Eng 2022;200:117715. https://doi.org/10.1016/j.applthermaleng.2021.117715.

[12] Yang J, Gao L, Ye Z, Hwang Y, Chen J. Binary-objective optimisation of latest low-GWP alternatives to R245fa for organic Rankine cycle application. Energy 2021;217:119336. https://doi.org/10.1016/j.energy.2020.119336.

[13] Javanshir A, Sarunac N, Razzaghpanah Z. Thermodynamic analysis of a regenerative organic Rankine cycle using dry fluids. Appl Therm Eng 2017;123:852–64. https://doi.org/10.1016/j.applthermaleng.2017.05.158.

[14] Liu W, Meinel D, Wieland C, Spliethoff H. Investigation of hydrofluoroolefins as potential working fluids in organic Rankine cycle for geothermal power generation. Energy 2014;67:106–16. https://doi.org/10.1016/j.energy.2013.11.081.

[15] Molés F, Navarro-Esbrí J, Peris B, Mota-Babiloni A, Mateu-Royo C. R1234yf and R1234ze as alternatives to R134a in Organic Rankine Cycles for low temperature heat sources. Energy Procedia 2017;142:1192–8. https://doi.org/10.1016/j.egypro.2017.12.380.

[16] Li J, Liu Q, Ge Z, Duan Y, Yang Z. Thermodynamic performance analyses and optimisation of subcritical and transcritical organic Rankine cycles using R1234ze (E) for 100–200 °C heat sources. Energy Convers Manag 2017;149:140–54. https://doi.org/10.1016/j.enconman.2017.06.060.

[17] Zhi LH, Hu P, Chen LX, Zhao G. Multiple parametric analysis, optimisation and efficiency prediction of transcritical organic Rankine cycle using trans-1,3,3,3-tetrafluoropropene (R1234ze(E)) for low grade waste heat recovery. Energy Convers Manag 2019;180:44–59. https://doi.org/10.1016/j.enconman.2018.10.086.

[18] Zhang X, Zhang Y, Cao M, Wang J, Wu Y, Ma C. Working fluid selection for organic Rankine cycle using single-screw expander. Energies (Basel) 2019;12:1–23. https://doi.org/10.3390/en12163197.

[19] Navarro-Esbrí J, Amat-Albuixech M, Molés F, Mateu-Royo C, Mota-Babiloni A, Collado R. HCFO-1224yd(Z) as HFC-245fa drop-in alternative in low temperature ORC systems: Experimental analysis in a waste heat recovery real facility. Energy 2020;193. https://doi.org/10.1016/j.energy.2019.116701.

[20] P. Haghparast, M. v. Sorin, M.A. Richard, H. Nesreddine, Analysis and design optimisation of an ejector integrated into an organic Rankine cycle, Appl Therm Eng. 159 (2019) 113979. https://doi.org/10.1016/j.applthermaleng.2019.113979.

[21] Rijpkema J, Andersson SB, Munch K. Experimental study of an organic Rankine cycle with R1233zd(E) for waste heat recovery from the coolant of a heavy-duty truck engine. Energy Convers Manag 2021;244:114500. https://doi.org/10.1016/j.enconman.2021.114500.

[22] Molés F, Navarro-Esbrí J, Peris B, Mota-Babiloni A, Kontomaris K. Thermodynamic analysis of a combined organic Rankine cycle and vapor compression cycle system activated with low temperature heat sources using low GWP fluids. Appl Therm Eng 2015;87:444–53. https://doi.org/10.1016/j.applthermaleng.2015.04.083.

[23] Yu H, Gundersen T, Feng X. Process integration of organic Rankine cycle (ORC) and heat pump for low temperature waste heat recovery. Energy 2018;160:330–40. https://doi.org/10.1016/j.energy.2018.07.028.

[24] Javanshir N, Seyed Mahmoudi SM, Rosen MA. Thermodynamic and exergoeconomic analyses of a novel combined cycle comprised of vapor-compression refrigeration and organic rankine cycles. Sustainability (Switzerland) 2019;11. https://doi.org/10.3390/su10023374.

[25] Liu L, Wu J, Zhong F, Gao N, Cui G. Development of a novel cogeneration system by combing organic rankine cycle and heat pump cycle for waste heat recovery. Energy 2021;217:119445. https://doi.org/10.1016/j.energy.2020.119445.

[26] Ashwni AF. Sherwani, Thermodynamic analysis of hybrid heat source driven organic Rankine cycle integrated flash tank vapor-compression refrigeration system. Int J Refrig 2021;129:267–77. https://doi.org/10.1016/j.ijrefrig.2021.05.006.

[27] Yang X, Zheng N, Zhao L, Deng S, Li H, Yu Z. Analysis of a novel combined power and ejector-refrigeration cycle. Energy Convers Manag 2016;108:266–74. https://doi.org/10.1016/j.enconman.2015.11.019.

[28] Pektezel O, Acar HI. Energy and exergy analysis of combined organic rankine cycle-single and dual evaporator vapor compression refrigeration cycle. Appl Sci (Switzerland) 2019;9. https://doi.org/10.3390/app9235028.

[29] Liao G, Liu L, Zhang F, Jiaqiang E, Chen J. A novel combined cooling-heating and power (CCHP) system integrated organic Rankine cycle for waste heat recovery of bottom slag in coal-fired plants. Energy Convers Manag 2019;186:380–92. https://doi.org/10.1016/j.enconman.2019.02.072.

[30] Nasir MT, Ekwonu MC, Esfahani JA, Kim KC. Performance assessment and multi-objective optimisation of an organic Rankine cycles and vapor compression cycle based combined cooling, heating, and power system. Sustain Energy Technol Assess 2021;47:101457. https://doi.org/10.1016/j.seta.2021.101457.

[31] Zhar R, Allouhi A, Ghodbane M, Jamil A, Lahrech K. Parametric analysis and multi-objective optimisation of a combined Organic Rankine Cycle and Vapor Compression Cycle. Sustain Energy Technol Assess 2021;47. https://doi.org/10.1016/j.seta.2021.101401.

[32] Eisavi B, Nami H, Yari M, Ranjbar F. Solar-driven mechanical vapor compression desalination equipped with organic Rankine cycle to supply domestic distilled water and power – Thermodynamic and exergoeconomic implications. Appl Therm Eng 2021;193:116997. https://doi.org/10.1016/j.applthermaleng.2021.116997.

[33] Sun W, Yue X, Wang Y. Exergy efficiency analysis of ORC (Organic Rankine Cycle) and ORC-based combined cycles driven by low-temperature waste heat. Energy Convers Manag 2017;135:63–73. https://doi.org/10.1016/j.enconman.2016.12.042.

[34] Wang L, Roskilly AP, Wang R. Solar Powered Cascading Cogeneration Cycle with ORC and Adsorption Technology for Electricity and Refrigeration. Heat Transfer Eng 2014;35:1028–34. https://doi.org/10.1080/01457632.2013.863067.

[35] Roumpedakis TC, Christou T, Monokrousou E, Braimakis K, Karellas S. Integrated ORC-Adsorption cycle: A first and second law analysis of potential configurations. Energy 2019;179:46–58. https://doi.org/10.1016/j.energy.2019.04.069.

[36] Lu F, Zhu Y, Pan M, Li C, Yin J, Huang F. Thermodynamic, economic, and environmental analysis of new combined power and space cooling system for waste heat recovery in waste-to-energy plant. Energy Convers Manag 2020;226. https://doi.org/10.1016/j.enconman.2020.113511.

[37] Zheng N, Wei J, Zhao L. Analysis of a solar Rankine cycle powered refrigerator with zeotropic mixtures. Sol Energy 2018;162:57–66. https://doi.org/10.1016/j.solener.2018.01.011.

[38] Saini P, Singh J, Sarkar J. Thermodynamic, economic and environmental analyses of a novel solar energy driven small-scale combined cooling, heating and power system. Energy Convers Manag 2020;226:113542. https://doi.org/10.1016/j.enconman.2020.113542.

[39] Demierre J, Henchoz S, Favrat D. Prototype of a thermally driven heat pump based on integrated Organic Rankine Cycles (ORC). Energy 2012;41:10–7. https://doi.org/10.1016/j.energy.2011.08.049.

[40] Liang Y, Mckeown A, Yu Z, Alshammari SFK. Experimental study on a heat driven refrigeration system based on combined organic Rankine and vapour compression cycles. Energy Convers Manag 2021;234:113953. https://doi.org/10.1016/j.enconman.2021.113953.

[41] Grauberger A, Young D, Bandhauer T. Experimental validation of an organic rankine-vapor compression cooling cycle using low GWP refrigerant R1234ze (E). Appl Energy 2022;307:118242. https://doi.org/10.1016/j.apenergy.2021.118242.

[42] Akbari Kordlar M, Mahmoudi SMS. Exergeoconomic analysis and optimisation of a novel cogeneration system producing power and refrigeration. Energy Convers Manag 2017;134:208–20. https://doi.org/10.1016/j.enconman.2016.12.007.

[43] Xia J, Wang J, Zhou K, Zhao P, Dai Y. Thermodynamic and economic analysis and multi-objective optimisation of a novel transcritical CO2 Rankine cycle with an ejector driven by low grade heat source. Energy 2018;161:337–51. https://doi.org/10.1016/j.energy.2018.07.161.

[44] Salim MS, Kim MH. Multi-objective thermo-economic optimisation of a combined organic Rankine cycle and vapour compression refrigeration cycle. Energy Convers Manag 2019;199. https://doi.org/10.1016/j.enconman.2019.112054.

[45] Cao Y, Dhahad HA, Hussen HM, Parikhani T. Proposal and evaluation of two innovative combined gas turbine and ejector refrigeration cycles fueled by biogas: Thermodynamic and optimisation analysis. Renew Energy 2022;181:749–64. https://doi.org/10.1016/j.renene.2021.09.043.

[46] Santiago TSA, Achiles AE, Dangelo JVH. Thermodynamic performance analysis and optimisation of a trigeneration system with different configurations applied to a medium-sized hospital. Energy 2022;239. https://doi.org/10.1016/j.energy.2021.122195.

[47] Al-Sayyab AKS, Navarro-Esbrí J, Mota-Babiloni A. Energy, exergy, and environmental (3E) analysis of a compound ejector-heat pump with low GWP refrigerants for simultaneous data center cooling and district heating. Int J Refrig 2021. https://doi.org/10.1016/j.ijrefrig.2021.09.036.

[48] S. Klein, Engineering Equation Solver (EES) V10.2., Fchart Software, Madison, USA. (2020). www.fchart.com.

[49] ASHRAE, Standard 34,designation and safety classification of refrigerants, 2019.

[50] Colmenar-Santos A, Folch-Calvo M, Rosales-Asensio E, Borge-Diez D. The geothermal potential in Spain. Renew Sustain Energy Rev 2016;56:865–86. https://doi.org/10.1016/j.rser.2015.11.070.

[51] A. Khalid, S. Al-Sayyab, A. Mota-Babiloni, Á. Barragán-Cervera, J. Navarro-Esbrí, Dual fluid trigeneration combined organic Rankine-compound ejector-multi evaporator vapour compression system, (n.d.). https://doi.org/10.1016/j.enconman.2022.115876.

[52] Liu X, Fu R, Wang Z, Lin L, Sun Z, Li X. Thermodynamic analysis of transcritical CO2 refrigeration cycle integrated with thermoelectric subcooler and ejector. Energy Convers Manag 2019;188:354–65. https://doi.org/10.1016/j.enconman.2019.02.088.

[53] Zhu Y, Li W, Wang Y, Li H, Li S. Thermodynamic analysis and parametric optimisation of ejector heat pump integrated with organic Rankine cycle combined cooling, heating and power system using zeotropic mixtures. Appl Therm Eng 2021;194:117097. https://doi.org/10.1016/j.applthermaleng.2021.117097.

[54] A. Khalid Shaker Al-Sayyab, A. Mota-Babiloni, J. Navarro-Esbrí, Novel compound waste heat-solar driven ejector-compression heat pump for simultaneous cooling and heating using environmentally friendly refrigerants, Energy Convers Manag.

228 (2021) 113703. https://doi.org/https://doi.org/10.1016/j.enconman.2020.113703.
[55] Xue X-D, Zhang T, Zhang X-L, Ma L-R, He Y-L, Li M-J, et al. Performance evaluation and exergy analysis of a novel combined cooling, heating and power (CCHP) system based on liquid air energy storage. Energy 2021;222:119975. https://doi.org/10.1016/j.energy.2021.119975.
[56] Kotas TJ. The Exergy Method of Thermal Plant Analysis. Elsevier 1985. https://doi.org/10.1016/C2013-0-00894-8.
[57] Rosen MA, Dincer I, Kanoglu M. Role of exergy in increasing efficiency and sustainability and reducing environmental impact. Energy Policy 2008;36:128–37. https://doi.org/10.1016/j.enpol.2007.09.006.
[58] Li Z, Li W, Xu B. Optimisation of mixed working fluids for a novel trigeneration system based on organic Rankine cycle installed with heat pumps. Appl Therm Eng 2016;94:754–62. https://doi.org/10.1016/j.applthermaleng.2015.10.145.
[59] Al-Sayyab AKS, Abdulwahid MA. Energy-exergy analysis of multistage refrigeration system and flash gas intercooler working with ozone-friendly alternative refrigerants to R134a. J Adv Res Fluid Mech Therm Sci 2019;63:188–98.
[60] Al-Sayyab AKS, Navarro-Esbrí J, Soto-Francés VM, Mota-Babiloni A. Conventional and Advanced Exergoeconomic Analysis of a Compound Ejector-Heat Pump for Simultaneous Cooling and Heating. Energies (Basel) 2021;14. https://doi.org/10.3390/en14123511.
[61] Bahadormanesh N, Rahat S, Yarali M. Constrained multi-objective optimisation of radial expanders in organic Rankine cycles by firefly algorithm. Energy Convers Manag 2017;148:1179–93. https://doi.org/10.1016/j.enconman.2017.06.070.
[62] Al-Sayyab AKS, Navarro-Esbrí J, Barragán-Cervera A, Mota-Babiloni A. Techno-economic analysis of a PV/T waste heat–driven compound ejector-heat pump for simultaneous data centre cooling and district heating using low global warming potential refrigerants. Mitig Adapt Strateg Glob Chang 2022;27:43. https://doi.org/10.1007/s11027-022-10017-6.